frontiers | Frontiers in Physics

ORIGINAL RESEARCH
published: 26 May 2022
doi: 10.3389/fphy.2022.893131

A Smartphone-Based Sensor With an Uncooled Infrared Thermal Camera for Accurate Temperature Measurement of Pig Groups

Fu Jiao[1,2†], Kun Wang[3†], Feng Shuang[1], Daming Dong[2] and Leizi Jiao[2]*

[1]Guangxi Key Laboratory of Intelligent Control and Maintenance of Power Equipment, Guangxi University, Nanning, China, [2]National Research Center of Intelligent Equipment for Agriculture, Beijing Academy of Agriculture and Forestry Sciences, Beijing, China, [3]State Key Laboratory of Remote Sensing Science, Aerospace Information Research Institute, Chinese Academy of Sciences, Beijing, China

Low-cost uncooled infrared thermal cameras show a large application potential for the rapid diagnosis of pig diseases. However, with the increase in ambient temperature and absorbing infrared radiation, almost all of them produce severe thermal drift and provide poor accuracy of temperature measurement. In addition, the unknown surface emissivity on a pig's body can also bring measuring errors. In this article, an uncooled infrared thermal camera with an accuracy of 3°C was used to develop a smartphone-based sensor for measuring the pig's temperature. Based on this sensor, we proposed a system combined with internal calibration for real-time compensation of the thermal drift and altering spectrum for eliminating the influence of unknown surface emissivity to improve the accuracy of temperature measurement. After calibration, the accuracy of this sensor was improved from 3 to 0.3°C without knowing the emissivity. We used this sensor to successfully identify pigs with abnormal temperatures on a livestock farm, which indicated that our proposed methods may be widely employed for rapid temperature screening and diagnosis of pig diseases.

Keywords: uncooled infrared thermal camera, temperature measurement accuracy, internal calibration, altering spectrum, rapid diagnosis of pig disease

OPEN ACCESS

Edited by:
Andrei Nomerotski, Brookhaven National Laboratory (DOE), United States

Reviewed by:
Ramy Abdlaty, McMaster University, Canada
Helmut Budzier, Technical University Dresden, Germany

***Correspondence:**
Leizi Jiao
jiaolz@nercita.org.cn

†These authors have contributed equally to this work and share first authorship

Specialty section:
This article was submitted to Radiation Detectors and Imaging, a section of the journal Frontiers in Physics

Received: *10 March 2022*
Accepted: *22 April 2022*
Published: *26 May 2022*

Citation:
Jiao F, Wang K, Shuang F, Dong D and Jiao L (2022) A Smartphone-Based Sensor With an Uncooled Infrared Thermal Camera for Accurate Temperature Measurement of Pig Groups. Front. Phys. 10:893131. doi: 10.3389/fphy.2022.893131

INTRODUCTION

Physiological abnormalities of pigs, such as fever, estrus, and skin rash, will lead to an abnormal change in the body temperature [1–4]. This change will occur earlier than other visible symptoms [5]. Therefore, an accurate measurement of temperature is important for the rapid diagnosis of pigs' physiological abnormalities [6–9]. At present, mercury-in-glass thermometers, ear tags, and infrared point thermometers are commonly used to measure pigs' body temperature. As a traditional method, a mercury-in-glass thermometer is accurate and inexpensive but easy to cause stress response and cross infection [10–13]. The ear tag allows continuous temperature measurements of pig groups. However, erroneous or failed temperature measurements will occur when the ear tags are loose or broken, owing to rubbing and gnawing between pigs [14, 15]. An infrared spot thermometer with non-contact and fast characteristics can effectively avoid stress response and cross infection. Nonetheless, its temperature measurement is easily affected by the local difference in the surface emissivity of pigs [16, 17], and all of these methods only measure temperature at one focal point of

the pig's body. Hyperspectral imaging can also be used as a reliable technique for the thermal measurement of biological tissues due to disease or thermal ablation treatment and has made some research progress [18, 19]. In the face of intensive farming with high population densities and numbers, a method that can quickly and accurately screen the pig's temperature is needed.

Infrared thermal imaging, as a new method for measuring temperature, has the advantages of non-contact and imaging measurement. These advantages make it possible to quickly screen the temperature of pig groups without stress [20, 21]. Over the years, considering the cost and portability, miniaturized low-cost uncooled infrared thermal cameras were used for applied research in multiple fields [22–24]. Based on a variety of uncooled infrared thermal cameras, researchers have identified the lameness, fever, estrus, and other activities, according to the temperature of pigs' backs, eyes, ear bases, auricles, and noses [25–29]. Although making a lot of progress, almost all of these works focus on the correlation between the body surface temperature and pig's health. Little attention has been paid to the temperature measurement accuracy of uncooled infrared thermal cameras. In one study of a pig's fever identification, Siewert et al. evaluated the characteristics of an uncooled infrared thermal camera used in their work and achieved a temperature measurement accuracy of ±2.0°C [30]. Traulsen et al. found that there were different errors when using the same uncooled infrared thermal camera to measure the temperature of the pigs' eyes, vulva, and ears [31]. Therefore, the accuracy of the uncooled infrared thermal camera actually cannot meet the need for an accurate measurement of the pig's surface temperature.

The thermal drift of an uncooled infrared thermal camera and the emissivity of an object are the two most influential factors of temperature measurement accuracy [32, 33]. With the increase in ambient temperature and absorbing infrared radiation, uncooled infrared thermal cameras produce severe thermal drift [34]. This is the main reason why almost all commercial uncooled infrared cameras have poor accuracy (about ± 3°C or even larger). In addition, our study showed that the surface emissivity between the different body parts of a pig is different [35]. The unknown emissivity also introduced measuring errors. Unfortunately, these two effects cannot be corrected by manually setting thermal camera parameters. Therefore, the external calibration system must be used to compensate for the influence of these two factors.

To measure the body surface temperature of an animal, the body surface emissivity must be known in advance, in the case of the IR thermal temperature measurement. However, the body surface emissivity of animals is affected by several factors, such as different surface stains, and the true emissivity of the body surface cannot be obtained. An altering spectrum system is a temperature measurement method based on monochromatic emissivity, which is unaffected by the difference in target emissivity and is usually achieved using IR filters to obtain IR thermal images in different wavelength bands [36, 37]. When measuring the temperature of high-temperature objects, the influence of surface emissivity on temperature measurement is usually attenuated by the altering spectrum method, which provides a reference. However, the applicability of this method for reducing the effect of variations in the body surface emissivity of a living animal at room temperature on the temperature measurement accuracy requires additional verification.

In this article, we developed a smartphone-based sensor using an uncooled infrared thermal camera with an accuracy of ±3°C for temperature measurement of pig groups on-site. To improve the accuracy of this sensor, we proposed a system combined with internal calibration and altering spectrum for real-time compensation of the thermal drift and eliminating the influence of unknown surface emissivity, respectively.

MATERIALS AND METHODS

Instruments and Materials

A schematic diagram of the sensor combined with the calibration system is shown in **Figure 1**. An uncooled infrared thermal camera (Therm-App, Opgal, Israel) with the response bands of 8–13 μm has a temperature measurement accuracy of ± 3°C. It was connected with a smartphone by a USB OTG interface for power supply and data transmission. The smartphone (Redmi

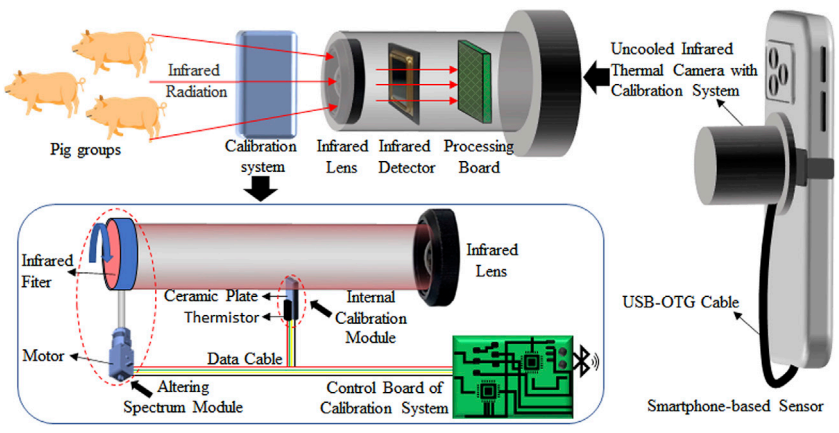

FIGURE 1 | Schematic diagram of the smartphone-based sensor combined with the calibration system for accurate temperature measurement of pig groups.

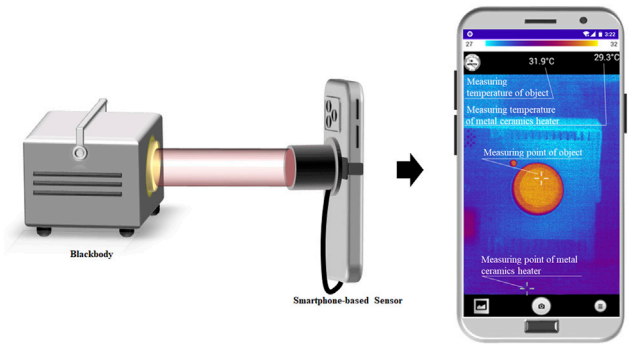

FIGURE 2 | Photo of the measuring process of $T_o^{'}$ and $T_m^{'}$ by our sensor.

Note 1, Xiaomi, China) running on an Android 4.4 system was used to acquire infrared thermal image data from this camera. It was also used to interact with the control board of the calibration system to set the ceramic plate temperature and rotate the infrared filter. The calibration system consists of three parts: the internal calibration module, altering spectrum module, and control board. APP software was developed on the smartphone for acquisition, control, and measurement. The control board can interact with the APP through Bluetooth communication and measure the environmental temperature. In addition, a black-body radiation source (Hyperion R-982, Isotech, Britain) was used to fit the compensation model for the calibration system.

In the internal calibration module, a micro constant temperature source is formed through a metal ceramics heater and a thermistor for the real-time correction of thermal drifts. The metal ceramic heater had an area of 15*10 mm^2 and was fixed in the front of the infrared lens. Using heat-dissipating silica gel, the thermistor adhered to one side of the metal ceramic heater facing away from the infrared lens. A temperature control accuracy of ±0.1°C was obtained by adjusting the current of the metal ceramic heater by using the control board, according to the value of the thermistor. In order to minimize the impact on the imaging function of the uncooled infrared thermal camera, only a small area of the micro constant temperature source entered the field of view of the infrared lens. The micro constant temperature source was set to 30°C during the whole calibration process.

TABLE 1 | T_e values obtained based on **Eq. 1** using the black-body source.

T_o (°C)	T_d (°C)
20< T_o <28	–1.6
28< T_o <31	–0.5
31< T_o <33	0.6
33< T_o <35	1.2
35< T_o <38	2.0
38< T_o <40	2.8
40< T_o <45	3.5

In the altering spectrum model, an infrared band pass filter with a diameter of 25.4 mm (Spectrogon, Taby, Sweden) was placed between the micro constant temperature source and the infrared lens. It has a pass band frequency of 9.48–10.093 μm and was fixed on a motor. The motor was driven by the control board and could be rotated freely. Therefore, infrared radiation in two different spectral bands could be obtained by moving in and out of the field of view of the infrared lens. It was used to verify the feasibility of the altering spectrum module for reducing the influence of the pig's body surface emissivity on temperature measurement accuracy.

Principle of Internal Calibration

Commercial uncooled infrared thermal cameras have a non-uniform correction model to ensure the response uniformity of all pixels of the detector [32, 33]. This provides us with a possibility to compensate the thermal drift of the detector by the calibration model of partial pixels. In our system of internal calibration, we assumed that the correction formula is defined as follows:

$$T_o = T_R + \left(T_m - T_m^{'}\right) + T_d. \quad (1)$$

Here, T_o is the true temperature of the object, T_R is the measured radiation temperature of the object by this sensor, T_m is the true temperature of the metal ceramic heater, and $T_m^{'}$ is the measured temperature of the metal ceramic heater. As the temperature of the object changes, the errors caused by the

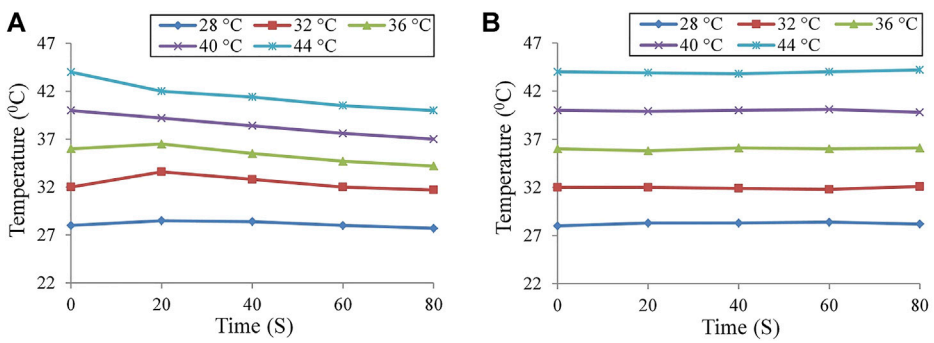

FIGURE 3 | Measured temperature of the black-body source changed with time by using our sensor: **(A)** before calibration and **(B)** after calibration by providing the internal calibration method. Reducing emissivity effect by the altering spectrum.

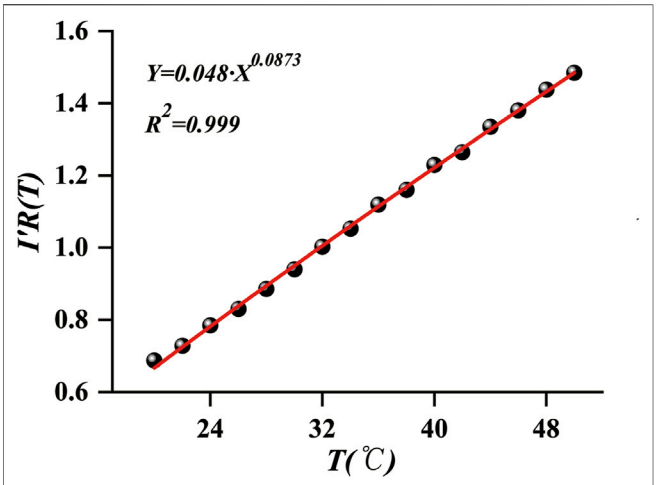

FIGURE 4 | Fitting curve of **Eq. 8** using the data by our sensor.

temperature drift response between the true and measured temperature may not remain constant. This difference in errors is expressed by T_d. When we set a different true temperature (T_o) of a black-body radiation source, $T_o^{'}$ *and* $T_m^{'}$ can be obtained by our sensor. T_m is also known. Therefore, T_d can be calculated by the data fitting process.

Principle of the Altering Spectrum

In the direct measurement of temperature, because the temperature and emissivity of the object are unknown, the emissivity must be measured before the temperature of the object can be calculated [14]. However, in the face of local differences among emissivity of pigskin, this direct method does not accurately detect temperature. The altering spectrum can simultaneously calculate the emissivity and true temperature of an object by obtaining the radiation temperature based on the infrared thermal camera in both spectral bands ($\Delta\lambda_1$ *and* $\Delta\lambda_2$)[38]. It can be expressed as follows [39]:

$$T_{R1}^{n1} = \varepsilon T_o^{n1} + (1-\varepsilon)T_u^{n1}, \tag{2}$$

$$T_{R2}^{n2} = \varepsilon T_o^{n2} + (1-\varepsilon)T_u^{n2}. \tag{3}$$

Here, ε is the emissivity of object, n_1 and n_2 are the power indexes in $\Delta\lambda_1$ *and* $\Delta\lambda_2$. T_{R2} (the measured radiation temperature of the object in $\Delta\lambda_1$), T_{R2} (the measured radiation temperature of the object in $\Delta\lambda_2$), and T_u (environmental temperature) can be detected by our sensor. In the bands of 8–13 um ($\Delta\lambda_1$, response bands of infrared cameras used in our sensor), n_1 = 3.9889[40]. Therefore, once n_2 corresponding to the infrared filter with the bands of 9.48–10.093 um ($\Delta\lambda_2$, bands of infrared filter used in our sensor) is obtained, the emissivity and (ε) and true temperature (T_o) of the object can be calculated by **Eqs 2**, **3**.

According to Planck's radiation law, the measured thermal radiation of the object by an infrared thermal camera is defined as follows:

$$I_R(T_o) = \int_{\Delta\lambda} R_\lambda L_{b\lambda}(T_o)d\lambda = \int_{\Delta\lambda} R_\lambda \frac{C_1}{\pi}\lambda^{-5}\left[exp\left(\frac{C_2}{\lambda T_o}\right)-1\right]^{-1}d\lambda. \tag{4}$$

Here, $L_{b\lambda}(T_o)$ is the spectral radiance of the object, R_λ is the spectral responsivity of the detector, and $\Delta\lambda$ is the spectral range of thermal radiation received by the camera. $C_1 = 3.7418 \times 10^{-4}(\mathrm{W}\cdot\mathrm{cm}^2)$ and $C_2 = 1.4388(\mathrm{cm}\cdot\mathrm{K})$ are the first and second radiative constants, respectively. Since R_λ is a constant for the same thermal infrared camera, **Eq. 4** can be simplified as follows [40]:

$$I_R(T_o) = \int_{\Delta\lambda} L_{b\lambda}(T_o)d\lambda \approx CT_o^n. \tag{5}$$

Here, C and n are variables that change with the spectral bands of infrared radiation received by the infrared thermal camera. When the spectral bands are $\Delta\lambda_1$ and $\Delta\lambda_2$ respectively, we can obtain the equation as follows:

$$I_{R_1}(T_o) = C_1 T_o^{n1}, \tag{6}$$

$$I_{R_2}(T_o) = C_2 T_o^{n2}. \tag{7}$$

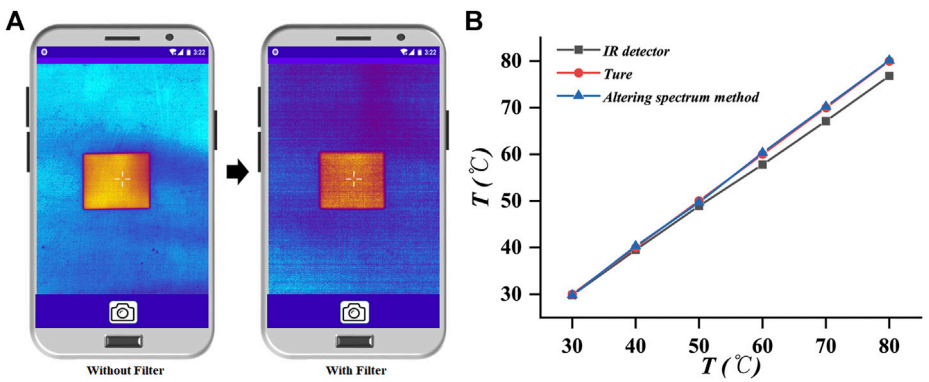

FIGURE 5 | Calibration result graph of the altering spectrum system. **(A)** Infrared thermal image of the paper before and after the addition of the filter. **(B)** True temperature of the paper, the temperature measured using the infrared detector, and the temperature measured using the altering spectrum system.

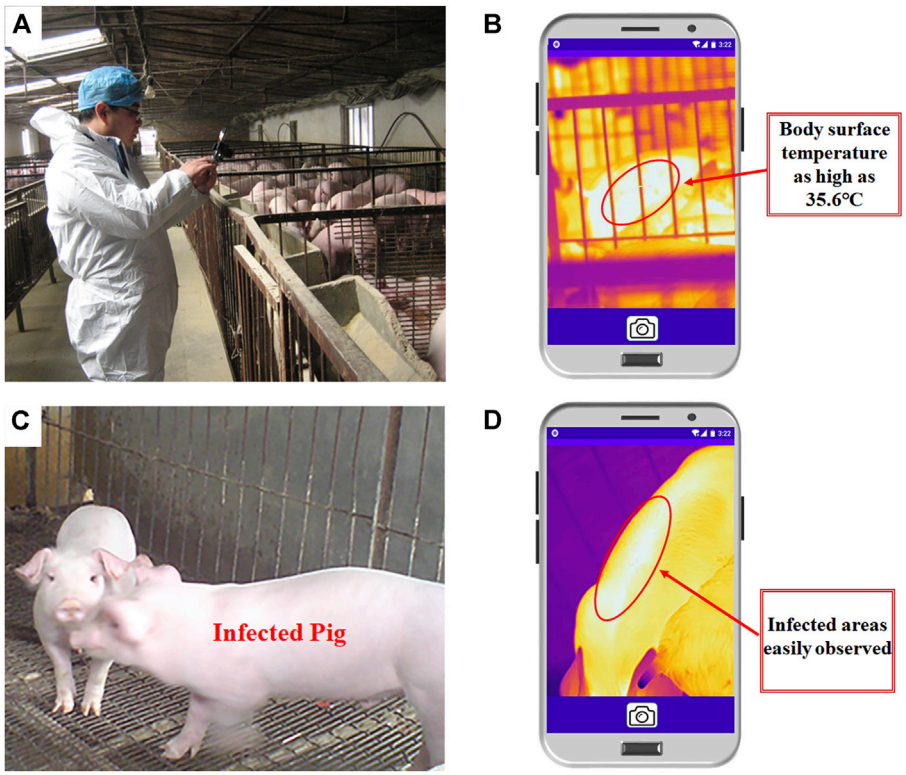

FIGURE 6 | Actual detection results. **(A,B)**: Infrared thermal images of the pigs suspected to be infected. **(A)** Actual detection process in the piggery. **(B)** Infrared thermal image of a suspected febrile pig. **(C)** Actual detection picture of the pigs where infectious diseases are frequent. **(D)** Infrared thermal image of a pig with an infectious disease.

By the ratio of **Eqs 6**, **7**, we obtain:

$$\frac{C_2 I_{R_1}(T_o)}{C_1 I_{R_2}(T_o)} = T_o^{n_1 - n_2}. \tag{8}$$

We define $\frac{I_{R_1}(T_o)}{I_{R_2}(T_o)} = I_R^{'}(T_o), \frac{C_2}{C_1} = C', and\ n_1 - n_2 = n'$; then, **Eq. 8** can be expressed as follows:

$$I_R^{'}(T_o) = C' T_o^{n'}. \tag{9}$$

Through measuring the infrared radiation corresponding to the different temperatures of the black-body source by our sensor, n_2 can be obtained based on **Eq. 8** or **Eq. 9**. On this basis, we can measure the true temperature of an object with unknown emissivity by our sensor based on **Eq. 2** and **Eq. 3**.

RESULTS AND DISCUSSION

Improving the Accuracy by the Internal Calibration

Considering the actual needs of a pig's temperature measurement, we set the object (black-body source) at different temperature values in the range of 25–45°C. Here, T_o and T_m are both given values; $T_o^{'}$ and $T_m^{'}$ could be measured by our sensor (as shown in **Figure 2**). Therefore, T_e was fitted in the range of 25–45°C based on **Eq. 1**, as shown in **Table 1**. It does not keep a constant and changes with the true temperature of the object.

Before using our internal calibration model (**Figure 3A**), we obtained the measured temperature of the black-body source with the true temperatures of 28, 32, 36, 40, and 44°C (**Figure 3A**). The measured temperature of the black-body source attenuates with time. The absolute errors between the measured and true temperature at different setting values were different but maintained a similar variation trend. In the range 35–42°C, we observed that the absolute errors were more than 2°C in 80 s. Therefore, the uncooled infrared thermal cameras used in our sensor could not accurately measure the pig's temperature without calibration. When our internal calibration module worked, our sensor re-measured the previous true temperature of the black-body source by using different T_e values. The curves are shown in **Figure 3B**. Compared with the results in **Figure 3A**, the measured temperature after calibration was almost equal to the true temperature of the black-body source. Moreover, the maximum error between measured and true temperature was only 0.4°C. These results indicated that the proposed internal calibration method could effectively correct the thermal drift of uncooled infrared thermal cameras.

In order to obtain the value of n_2, the temperature of the black-body source was set from 20 to 50°C with an increment of 2°C. **Eq. 9** could be fitted by the data acquired by our sensor when the infrared filter moved in and out of the field of view of the infrared lens (**Figure 4**). Here, we observed $n' = 0.0873$; thus, $n_2 = n_1 - n' = 3.0916$. According to **Eqs 2**, **3**, our sensor could

measure the true temperature of the object with unknown emissivity.

To verify the reliability of the altering spectrum for improving the accuracy of temperature measurement, we used white paper as a test object. The paper was tightly placed on a heated platform with a temperature-controlled system. At this point, the temperature of the platform was the true temperature of the paper. **Figure 5A** shows the thermal images before and after the addition of the filter. The thermal images were relatively clear and showed a high quality when no filter was added, whereas the imaging quality deteriorated after the addition of the filter. This change is attributed to the decrease in the IR radiation received from the detector. Subsequently, the temperatures of the temperature control platform were set to 30, 40, 50, 60, 70, and 80°C. After the temperature of the paper was stabilized, the measurements were taken separately. **Figure 5B** shows the variation between the true temperatures of the paper, the temperature measured using the IR detector, and the temperature measured using the altering spectrum system before and after the addition of the filter. Apparently, the temperature measured directly through the IR detector deviates from the true temperature by receiving the influence of the emissivity of the paper surface. Using the temperature of the paper obtained using the altering spectrum temperature measurement system is highly consistent with the true temperature, with a maximum error of only 0.3°C. Thus, the altering spectrum system can effectively eliminate the effect of unknown emissivity and improve the temperature measurement accuracy of the system.

Application

We used our sensor to conduct a random body surface temperature screening of normal pigs housed in 12 rooms (6 pigs in each room) on the farm. As shown in **Figure 6A**, a staff used our sensor to screen the body temperature of pig groups on-site. The thermal image (**Figure 6B**) showed that the abdomen's temperature of one pig was higher than that of others, which indicated that the pig might be febrile. After identifying artificially, the rectal temperature of the pig was up to 41°C, with the possibility of fever.

In addition, one thermal image was obtained from a pig hen where an infectious skin disease was prevalent (The sick pig was kept in a separate room from another pig with the same skin disease), and visible images and visual observation could not be distinguished between infected and uninfected pigs (**Figure 6C**). However, when the proposed temperature measurement system was used for detection, pigs with abnormal body surface temperatures were clearly observed in the IR images (**Figure 6D**). Therefore, our sensor could quickly and accurately screen the body surface temperature of pig groups and isolate animals with abnormal temperatures promptly, thereby effectively controlling the spread of diseases in livestock and poultry houses.

CONCLUSION

In summary, we present a smartphone-based sensor with an uncooled infrared thermal camera. We demonstrated that the internal calibration system designed around the infrared camera can effectively suppress the temperature measurement errors induced by the detector's response drift. Moreover, the altering spectrum temperature measurement system designed can achieve high-precision, real-time temperature measurements when the target emissivity is unknown. This facilitates the effective elimination of temperature measurement errors induced by surface emissivity. Furthermore, the robust and accurate population temperature measurement capability of the system is verified based on the measurements conducted on pig populations in a piggery. The proposed system can be an effective temperature screening tool and shows considerable potential for application in animal population health control and early disease prevention.

DATA AVAILABILITY STATEMENT

The original contributions presented in the study are included in the article/supplementary material; further inquiries can be directed to the corresponding author.

ETHICS STATEMENT

Ethical review and approval were not required for the animal study because the pigs in the *Applications Section* of our submitted manuscript are from the farm of Beijing Xinliu Agriculture and Animal Husbandry Technology Co. This farm has a lot of long-term cooperation with our institution. Our experiments were also carried out with the approval of the farm owner. The measurement process was under the guidance of professional farm personnel. Due to the unique advantages of our designed sensors, the entire measurement process was performed without direct contact with the animal body. More importantly, there was no harm or abuse to the animal body, and the pigs with fever or disease detected during the experiment were found naturally without human intervention.

AUTHOR CONTRIBUTIONS

All authors listed have made a substantial, direct, and intellectual contribution to the work and approved it for publication.

FUNDING

This research was financially supported by the National Key R&D Program of China (2021ZD0113801), the Natural Science Foundation of China under Grant (61720106009), the Distinguished Young Scientists Program of Beijing Natural Science Foundation (JQ19023), and National & Local Joint Engineering Laboratory For Agricultural Internet of Things (PT2022-23).

REFERENCES

1. Randi F, McDonald M, Duffy P, Kelly AK, Lonergan P. The Relationship between External Auditory Canal Temperature and Onset of Estrus and Ovulation in Beef Heifers. *Theriogenology* (2018) 110:175–81. doi:10.1016/j.theriogenology.2018.01.001
2. Ricci A, Racioppi V, Iotti B, Bertero A, Reed KF, Pascottini OB, et al. Assessment of the Temperature Cut-Off point by a Commercial Intravaginal Device to Predict Parturition in Piedmontese Beef Cows. *Theriogenology* (2018) 113:27–33. doi:10.1016/j.theriogenology.2018.02.009
3. Glassman SD, Carreon LY, Aruwajoye O, Benson NM, Li P, Kurian AS. Local Temperature Elevation as a Marker of Spinal Implant Infection in an Animal Model. *North Am Spine Soc J (Nassj)* (2021) 7:100077. doi:10.1016/j.xnsj.2021.100077
4. Abdlaty R, Hayward J, Farrell T, Fang Q. Skin Erythema and Pigmentation: a Review of Optical Assessment Techniques. *Photodiagnosis Photodynamic Ther* (2021) 33:102127. doi:10.1016/j.pdpdt.2020.102127
5. Postel A, Austermann-Busch S, Petrov A, Moennig V, Becher P. Epidemiology, Diagnosis and Control of Classical Swine Fever: Recent Developments and Future Challenges. *Transbound Emerg Dis* (2018) 65:248–61. doi:10.1111/tbed.12676
6. Sathiyabarathi M, Jeyakumar S, Manimaran A, Jayaprakash G, Pushpadass HA, Sivaram M, et al. Infrared Thermography: A Potential Noninvasive Tool to Monitor Udder Health Status in Dairy Cows. *Vet World* (2016) 9:1075–81. doi:10.14202/vetworld.2016.1075-1081
7. Sejian V, Bhatta R, Gaughan JB, Dunshea FR, Lacetera N. Review: Adaptation of Animals to Heat Stress. *Animal* (2018) 12:s431–s444. doi:10.1017/s1751731118001945
8. Sinha R, Bhakat M, Mohanty T, Ranjan A, Kumar R, Lone SA, et al. Infrared Thermography as Non-invasive Technique for Early Detection of Mastitis in Dairy Animals-A Review. *Asian J Dairy Food Res* (2018) 37:1–6. doi:10.18805/ajdfr.R-1746
9. Nääs IA, Garcia RG, Caldara FR. Infrared thermal Image for Assessing Animal Health and Welfare. *J Anim Behav Biometeorology* (2020) 2:66–72.
10. Stewart M, Webster JR, Verkerk GA, Schaefer AL, Colyn JJ, Stafford KJ. Non-invasive Measurement of Stress in Dairy Cows Using Infrared Thermography. *Physiol Behav* (2007) 92:520–5. doi:10.1016/j.physbeh.2007.04.034
11. Herborn KA, Graves JL, Jerem P, Evans NP, Nager R, McCafferty DJ, et al. Skin Temperature Reveals the Intensity of Acute Stress. *Physiol Behav* (2015) 152:225–30. doi:10.1016/j.physbeh.2015.09.032
12. Herborn KA, Jerem P, Nager RG, McKeegan DEF, McCafferty DJ. Surface Temperature Elevated by Chronic and Intermittent Stress. *Physiol Behav* (2018) 191:47–55. doi:10.1016/j.physbeh.2018.04.004
13. Ricci GD, Silva-Miranda KOd., Titto CG. Infrared Thermography as a Non-invasive Method for the Evaluation of Heat Stress in Pigs Kept in Pens Free of Cages in the Maternity. *Comput Electro Agric* (2019) 157:403–9. doi:10.1016/j.compag.2019.01.017
14. Bernard V, Staffa E, Mornstein V, Bourek A. Infrared Camera Assessment of Skin Surface Temperature - Effect of Emissivity. *Physica Med* (2013) 29:583–91. doi:10.1016/j.ejmp.2012.09.003
15. Harrap MJM, Hempel de Ibarra N, Whitney HM, Rands SA. Reporting of Thermography Parameters in Biology: a Systematic Review of thermal Imaging Literature. *R Soc Open Sci* (2018) 5:181281. doi:10.1098/rsos.181281
16. Jara AL, Hanson JM, Gabbard JD, Johnson SK, Register ET, He B, et al. Comparison of Microchip Transponder and Noncontact Infrared Thermometry with Rectal Thermometry in Domestic Swine (*Sus scrofa* Domestica). *J Am Assoc Lab Anim Sci* (2016) 55:588–93.
17. Kritchevsky J. Forensic Physical Examination of Large Animals. *Vet Forensics* (2017) 153–86. doi:10.4324/9781315153421-6
18. Abdlaty R, Doerwald-Munoz L, Farrell TJ, Hayward JE, Fang Q. Hyperspectral Imaging Assessment for Radiotherapy Induced Skin-Erythema: Pilot Study. *Photodiagnosis Photodynamic Ther* (2021) 33:102195. doi:10.1016/j.pdpdt.2021.102195
19. De Landro M, Saccomandi P, Barberio M, Schena E, Marescaux M, Diana M. *Hyperspectral Imaging for thermal Effect Monitoring in* in Vivo *Liver during Laser Ablation*. IEEE (2019). p. 1851–4.
20. McManus C, Tanure CB, Peripolli V, Seixas L, Fischer V, Gabbi AM, et al. Infrared Thermography in Animal Production: An Overview. *Comput Electro Agric* (2016) 123:10–6. doi:10.1016/j.compag.2016.01.027
21. Tattersall GJ. Infrared Thermography: A Non-invasive Window into thermal Physiology. *Comp Biochem Physiol A: Mol Integr Physiol* (2016) 202:78–98. doi:10.1016/j.cbpa.2016.02.022
22. Brooks JP, Brooks JM, Seals T. Smartphone thermal Imaging in the Detection of Testicular Ischemia. *Urology* (2021) 157:233–8. doi:10.1016/j.urology.2021.02.031
23. Coşkun G, Aytekin İ. Early Detection of Mastitis by Using Infrared Thermography in Holstein-Friesian Dairy Cows via Classification and Regression Tree (CART) Analysis. *Selcuk J Agric Food Sci* (2021) 35:115–24. doi:10.15316/SJAFS.2021.237
24. González-Pérez S, Perea Ström D, Arteaga-Marrero N, Luque C, Sidrach-Cardona I, Villa E, et al. Assessment of Registration Methods for thermal Infrared and Visible Images for Diabetic Foot Monitoring. *Sensors* (2021) 21:2264. doi:10.3390/s21072264
25. D.S. L, Jeyakumar S, Vasant PJ, Sathiyabarathi M, Manimaran A, Kumaresan A, et al. Monitoring Foot Surface Temperature Using Infrared thermal Imaging for Assessment of Hoof Health Status in Cattle: A Review. *J Therm Biol* (2018) 78:10–21. doi:10.1016/j.jtherbio.2018.08.021
26. de Ruediger FR, Yamada PH, Bicas Barbosa LG, Mungai Chacur MG, Pinheiro Ferreira JC, de Carvalho NAT, et al. Effect of Estrous Cycle Phase on Vulvar, Orbital Area and Muzzle Surface Temperatures as Determined Using Digital Infrared Thermography in buffalo. *Anim Reprod Sci* (2018) 197:154–61. doi:10.1016/j.anireprosci.2018.08.023
27. Narayan E, Perakis A, Meikle W. Using Thermal Imaging to Monitor Body Temperature of Koalas (*Phascolarctos cinereus*) in A Zoo Setting. *Animals* (2019) 9:1094. doi:10.3390/ani9121094
28. Santiago PR, Martínez-Burnes J, Mayagoitia AL, Ramírez-Necoechea R, Mota-Rojas D. Relationship of Vitality and Weight with the Temperature of Newborn Piglets Born to Sows of Different Parity. *Livestock Sci* (2019) 220:26–31. doi:10.1016/j.livsci.2018.12.011
29. Zhang Z, Zhang H, Liu T. Study on Body Temperature Detection of Pig Based on Infrared Technology: A Review. *Artif Intelligence Agric* (2019) 1:14–26. doi:10.1016/j.aiia.2019.02.002
30. Siewert C, Dänicke S, Kersten S, Brosig B, Rohweder D, Beyerbach M, et al. Difference Method for Analysing Infrared Images in Pigs with Elevated Body Temperatures. *Z für Medizinische Physik* (2014) 24:6–15. doi:10.1016/j.zemedi.2013.11.001
31. Traulsen I, Naunin K, Müller K, Krieter J. Untersuchungen zum Einsatz der Infrarotthermographie zur Messung der Körpertemperatur bei Sauen. *Zuchtungskunde* (2010) 82(6):437–446.
32. Yanming Q, Hao X, Zhiyong K. Research on Some Influence Factors in High Temperature Measurement of Metal with thermal Infrared Imager. *Phys Proced* (2011) 19:207–13. doi:10.1016/j.phpro.2011.06.150
33. Fernández-Cuevas I, Bouzas Marins JC, Arnáiz Lastras J, Gómez Carmona PM, Piñonosa Cano S, García-Concepción MÁ, et al. Classification of Factors Influencing the Use of Infrared Thermography in Humans: A Review. *Infrared Phys Techn* (2015) 71:28–55. doi:10.1016/j.infrared.2015.02.007
34. Liang K, Yang C, Peng L, Zhou B. Nonuniformity Correction Based on Focal Plane Array Temperature in Uncooled Long-Wave Infrared Cameras without a Shutter. *Appl Opt* (2017) 56:884–9. doi:10.1364/ao.56.000884
35. Zhang K, Jiao L, Zhao X, Dong D. An Instantaneous Approach for Determining the Infrared Emissivity of Swine Surface and the Influencing Factors. *J Therm Biol* (2016) 57:78–83. doi:10.1016/j.jtherbio.2016.03.003
36. Hijazi A, Sachidanandan S, Singh R, Madhavan V. A Calibrated Dual-Wavelength Infrared Thermometry Approach with Non-greybody Compensation for Machining Temperature Measurements. *Meas Sci Technol* (2011) 22:025106. doi:10.1088/0957-0233/22/2/025106
37. McLean AG, Ahn J-W, Maingi R, Gray TK, Roquemore AL. A Dual-Band Adaptor for Infrared Imaging. *Rev Scientific Instr* (2012) 83:053706. doi:10.1063/1.4717672

38. Inagaki T, Okamoto Y, Fan Z, Kurokawa K. Temperature Measurement and Accuracy of Bi-colored Radiometer Applying Pseudo Graybody Approximation. *SPIE* (1994) 2245:274–85. doi:10.1117/12.171177
39. Gaussorgues G, Chomet S. *Infrared Thermography*. Springer Science & Business Media (1993).
40. Inagaki T, Okamoto Y. Surface Temperature Measurement Near Ambient Conditions Using Infrared Radiometers with Different Detection Wavelength Bands by Applying a Grey-Body Approximation: Estimation of Radiative Properties for Non-metal Surfaces. *NDT E Int* (1996) 29:363–9. doi:10.1016/s0963-8695(96)00039-4

Conflict of Interest: The authors declare that the research was conducted in the absence of any commercial or financial relationships that could be construed as a potential conflict of interest.

Publisher's Note: All claims expressed in this article are solely those of the authors and do not necessarily represent those of their affiliated organizations, or those of the publisher, the editors, and the reviewers. Any product that may be evaluated in this article, or claim that may be made by its manufacturer, is not guaranteed or endorsed by the publisher.